Stability analysis of two-layer immiscible viscous fluids in an inclined closed tube

Zhan Wang
University of Wisconsin

The present investigation is concerned with the role of bottom slope in the stability properties of two-dimensional disturbances in sheared two-layer immiscible fluids with stepwise densities. A linear analysis of normal mode instability of the interface in an inclined closed tube is carried out using full Navier-Stokes equation using Chebyshev-tau method. It has been observed that Reynolds number and the tilt angle both have destabilizing effect on the interface eigenvalue problem of Orr-Sommerfeld equation. As a special example, Stokes flow is proven to be stable for any angles. A weakly nonlinear model equation, which is Kuramoto-Sivashinsky type, for the interface is given using multi-scale method, and the long wave dispersion relation gives a sufficient condition for triggering the instability.

1 Introduction

When two fluids of different physical properties are superposed one over the other and are moving with a relative horizontal velocity, the instability occurs at the interface. Two-layer fluids are ubiquitous in both ocean and atmosphere such as the exchange of Atlantic Ocean water with the saltier Mediterranean Sea water through the Strait of Gibralta, light water entering the ocean space from a suddenly broken dam, rapid melting of continental ice, mixing of clouds and etc. The seminal paper on experimental results for two-layer fluid was carried out by Thorpe (1968,1971) for the continuously stratified mixing fluids with acceleration share profile called Kelvin-Helmholtz instability, which revealed the relationship between the lab experiment and the real instability and turbulence in the ocean and atmosphere.

Theoretical approaches for layered viscous channel flow often consider the stability of a basic flow to normal mode type disturbances. The first theoretical study appears to have been a paper by Yih (1967) who discussed the linear stability of two-layer Couette and plane Poiseuille flows using a long-wave approach. He showed that both viscosity and density stratification can generate an interfacial instability, recognized as Kelvin-Helmholtz instability which was also called the interfacial mode, at any Reynolds number. A different, shear type instability mechanism has been found by Hooper & Boyd (1983) occurring primarily for short waves at small Reynolds number. The stability properties at intermediate wavelengths are complicated by mode crossings. Accurate numerical stability studies for the two-layer Orr-Sommerfeld equations (linearized Navier-Stokes) can be implemented recently since the Chebyshev-tau method was developed by Dongarra *et al* (1996) and Boomkamp *et al* (1997). There is a large number of literature in both mixing layers and immiscible

fluids for plane channel flows, reader is referred to Hooper & Grimshaw (1985), Yiantsios & Higgins (1988), Pozrikidis (1997), Yecko *et al* (2002), Bague *et al* (2010), Bassom *et al* (2010), Mählmann & Papageorgiou (2010) and the references therein.

Since the instability between two fluids is generated by unbalanced pressure resulting from the perturbation of the velocity shear flow, the combination of external forcing and topographic features, such as sloping bottom, on a two-layer baroclinic flow results in various types of instabilities at the interface. The first paper for viscous fluid moving down an inclined plane was proposed by Yin (1963), which firstly clarified the boundary conditions on the free surface of one layer fluid. Kao (1965) gave the linear analysis for two-layer Poiseuille flow with a sloping bottom in the presence of both interface and free surface using long wave approximation. More recently, Defina *et al* (1999) considered the viscous effect in an inclined tube for the fluid with continuously stratified density, and Negretti (2008) presented more numerical results for an inclined stratified shear flow under Boussinesq assumption. On the experimental side, besides Thorpe's famous work in 70's, Fouli & Zhu (2011) performed a new experiment to understand the generation conditions and development of Kelvin-Helmholtz instabilities in two-layer exchange flows downslope of a bottom sill. The low frequency oscillation were observed to led to the development of large-scale downslope waves that caused significant interfacial entrainment.

Reduced potential models for those fluids which the vorticity is identically zero, and the velocity is thus given by the gradient of a harmonic potential, have also been developed to study the interface stability problem in multi-layer fluids. Purely inviscid potential flow is the simplest nonlinear model, and the vortex sheet method or called boundary integral method is a successful numerical method to simulate the Kelvin-Helmohltz instability (see [14] and the references therein). There are two theories of potential flow of a viscous fluid: viscous potential flow and the dissipation method. In the viscous potential theory, the effects of viscosity on the normal stress are not neglected but the effect of shear stresses are neglected, in other words, the governing equation is Laplace while the viscosity enters through normal stress balance and tangential stresses are not considered on the interface. On the other hand, the dissipative method is a famous theory which was first introduced by Stokes in his study of the decay waves, which based on the basic fact that the viscous stresses of the irrotational flow are self-equilibrated and do not give rise to forces in the equations but they do work and give rise to energy and dissipation. In a recent paper, Kim *et al* (2011) used the linearized versions of these models to the research of Kelvin-Helmohltz instability.

This work concerns two-layer immiscible fluids in an inclined closed tube and has been extended Thorpe's classic work to the viscous and non-mixing case. The aim of the present linear stability study is to examine the influence of a bottom slope on the stability of the interface under the action of a shear advection. The bottom slope has destabilizing effect of buoyancy at the interface and adds an additional acceleration term which results in a parabola base shear flow. It is much natural than the plane channel flow which needs extra force to maintain the base shear and more realistic in the case of oil & water interface. The primary problem to which we shall address the following analysis is the investigation of the static stability of the interface y=0 in the tilt coordinates between two parallel shear flows $U_{1,2}(y)$ of a light viscous incompressible fluid in y>0 and a heavy one in y<0 when this interface is subjected to the small periodic perturbation.

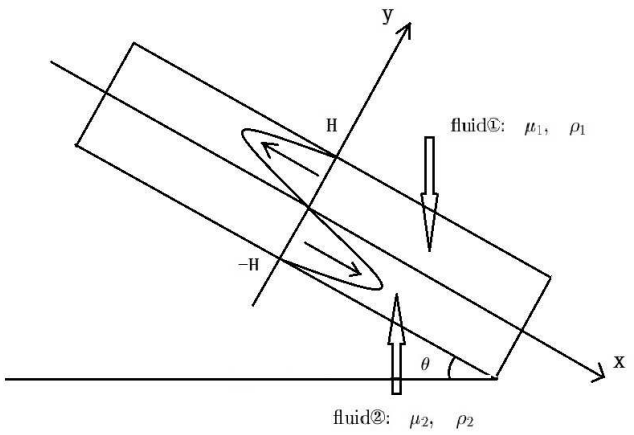

Figure 1: Schematic sketch in tilt coordinates of two-layer viscous fluids with parabolic shear flow.

The rest of the paper is organized as follows. In Sec. II the base shear flow is calculated and the governing equations and the connecting boundary conditions on the interface for the perturbed system are presented. In Sec. III, the Chebyshev-tau method is applied to solve the eigenvalue problem for two-layer Orr-Sommerfeld systems. The results for both Stokes flow and general case are discussed for the additional effect of changing the density ratio, tilt angle, surface tension and Reynolds number. In Sec. IV, a weakly nonlinear PDE model for the long wave perturbation is derived via multi-scale method, and a sufficient condition for generating instability is also obtained automatically. Finally, Sec. V summarizes the results and includes conclusion.

2 Formulation

2.1 Governing equation

The flow is assumed to be viscous, incompressible fluids at uniform depth inclined tube at an angle θ in a gravitational field with the coordinate axes $x-y$ as shown in Fig.1 with origin at the interface. The upper layer is a fluid of density ρ_1 and the lower layer is of density ρ_2 with $\rho_2 > \rho_1$. The governing Navier-Stokes equations (NSE) in the tilt coordinates read

$$\frac{\partial \widetilde{u}_i}{\partial t} + \widetilde{u}_i \frac{\partial \widetilde{u}_i}{\partial x} + \widetilde{v}_i \frac{\partial \widetilde{u}_i}{\partial y} = -\frac{1}{\rho_i}\frac{\partial \widetilde{P}_i}{\partial x} + g\sin\theta + \frac{\mu_i}{\rho_i}\nabla^2 \widetilde{u}_i \tag{1}$$

$$\frac{\partial \widetilde{v}_i}{\partial t} + \widetilde{u}_i \frac{\partial \widetilde{v}_i}{\partial x} + \widetilde{v}_i \frac{\partial \widetilde{v}_i}{\partial y} = -\frac{1}{\rho_i}\frac{\partial \widetilde{P}_i}{\partial y} - g\cos\theta + \frac{\mu_i}{\rho_i}\nabla^2 \widetilde{v}_i \tag{2}$$

$$\frac{\partial \widetilde{u}_i}{\partial x} + \frac{\partial \widetilde{v}_i}{\partial y} = 0 \tag{3}$$

where $i = 1, 2$ denotes two different fluids. $\widetilde{u}, \widetilde{v}$ are the velocities in x and y directions respectively, $\widetilde{P}$ is the pressure and μ_i represents the dynamic viscosity. For the closed tube, the base shear flow profiles take the form

$$\widetilde{u}_1 = \frac{(1-\gamma)g}{1+m^2+14m}\frac{\rho_2}{\mu_2}\sin\theta\Big[\frac{7+m}{2}y^2 - 4Hy + \frac{1-m}{2}H^2\Big] \tag{4}$$

$$\widetilde{u}_2 = \frac{(1-\gamma)g}{1+m^2+14m}\frac{\rho_2}{\mu_2}\sin\theta\Big[-\frac{7m+1}{2}y^2 - 4mHy + \frac{1-m}{2}H^2\Big] \tag{5}$$

where $m \triangleq \frac{\mu_1}{\mu_2}$ is the dynamic viscosity ratio, and $\gamma \triangleq \frac{\rho_1}{\rho_2}$ is the density ratio. In the mean time $\widetilde{v}_1 = \widetilde{v}_2 = 0$. Defining $g' \triangleq \frac{\rho_2-\rho_1}{\rho_2}g = (1-\gamma)g$ as the reduced gravity, then we can define the typical velocity scale as

$$U \triangleq \frac{g'}{1+m^2+14m}\frac{\rho_2}{\mu_2}\sin\theta \tag{6}$$

Introducing dimensionless variables that are constructed using the velocity scale, U, and the length scale, H, we find that the problem is characterized by the Reynolds number, R_i, the Froude number, F, the surface tension parameter, S. More precisely, rescaling the system by

$$\big(\widetilde{u}_i, \widetilde{v}_i\big) = U\big(u_i', v_i'\big), \quad \big(x, y\big) = H\big(x', y'\big), \quad \widetilde{P}_i = \rho_i U^2 P_i', \quad t = \frac{H}{U}t' \tag{7}$$

With a little abuse of notation, we still use (t,x,y) as the time and space coordinates for simplicity, then the governing equations are of the form

$$\frac{\partial u_i'}{\partial t} + u_i'\frac{\partial u_i'}{\partial x} + v_i'\frac{\partial u_i'}{\partial y} = -\frac{\partial P_i'}{\partial x} + \frac{\sin\theta}{F^2} + \frac{1}{R_i}\nabla^2 u_i' \tag{8}$$

$$\frac{\partial v_i'}{\partial t} + u_i'\frac{\partial v_i'}{\partial x} + v_i'\frac{\partial v_i'}{\partial y} = -\frac{\partial P_i'}{\partial y} - \frac{\cos\theta}{F^2} + \frac{1}{R_i}\nabla^2 v_i' \tag{9}$$

$$\frac{\partial u_i'}{\partial x} + \frac{\partial v_i'}{\partial y} = 0 \tag{10}$$

Here $R_i = \frac{\rho_i HU}{\mu_i}$ is Reynolds number, $F = \frac{U}{(gH)^{1/2}}$ is Froude number, and for later use, the dimenionless surface tension is defined as $S = \frac{\sigma}{\rho_2 HU^2}$, where σ is the coefficient of surface tension (assumed constant). Furthermore, we have

$$\frac{R_2}{F^2} = \frac{\rho_2 HU}{\mu_2}\cdot\frac{gH}{U^2} = \frac{1+m^2+14m}{1-\gamma}\frac{1}{\sin\theta} \tag{11}$$

$$R_2 S = \frac{\rho_2 HU}{\mu_2}\cdot\frac{\sigma}{\rho_2 HU^2} = \frac{(1+m^2+14m)\sigma}{\rho_2 g' H^2\sin\theta} \tag{12}$$

Finally, we can rewrite the base shear flow as

$$U_1 = \frac{\widetilde{u}_1}{U} = \frac{7+m}{2}y^2 - 4y + \frac{1-m}{2} \tag{13}$$

$$U_2 = \frac{\widetilde{u}_2}{U} = -\frac{7m+1}{2}y^2 - 4my + \frac{1-m}{2} \tag{14}$$

2.2 Linearization

Assuming small perturbations from the basic flow in the form,

$$u_i' = U_i(y) + u_i, \quad v_i' = v_i, \quad P_i' = P_i(x,y) + p_i \tag{15}$$

neglecting second order terms in the primed quantities, and making use of the fact that U_i and P_i satisfy the basic flow equations, we have, upon substitution of (15) into (8)-(10), the linearized equations governing the disturbance motion,

$$\frac{\partial u_i}{\partial t} + U_i\frac{\partial u_i}{\partial x} + DU_i v_i = -\frac{\partial p_i}{\partial x} + \frac{1}{R_i}\nabla^2 u_i \tag{16}$$

$$\frac{\partial v_i}{\partial t} + U_i\frac{\partial v_i}{\partial x} = -\frac{\partial p_i}{\partial y} + \frac{1}{R_i}\nabla^2 v_i \tag{17}$$

$$\frac{\partial u_i}{\partial x} + \frac{\partial v_i}{\partial y} = 0 \tag{18}$$

where the operator D means the derivative with respect to y. No-slip and no-penetration boundary conditions are posed on the two fixed walls for the perturbation

$$u_1(t,x,1) = Du_1(t,x,1) = u_2(t,x,-1) = Du_2(t,x,-1) = 0 \tag{19}$$

Suppose the perturbation of the interface is designated as $y = \eta(t,x)$, then on the interface, the boundary conditions are as follows

- contiunity of velocity: $u_1' = u_2'$, $v_1' = v_2'$
- contiunity of tangential stress: $\mu_1\Big(\frac{\partial v_1'}{\partial x} + \frac{\partial u_1'}{\partial y}\Big) = \mu_2\Big(\frac{\partial v_2'}{\partial x} + \frac{\partial u_2'}{\partial y}\Big)$
- contiunity of normal stress: $\big(-P_2' + \frac{2}{R_2}\frac{\partial v_2'}{\partial y}\big) - \gamma\big(-P_1' + \frac{2}{R_1}\frac{\partial v_1'}{\partial y}\big) - S\frac{\partial^2\eta}{\partial x^2} = 0$

For two-dimensinal incompressible Navier-Stokes equation, it is convenient to introduce the stream function Ψ_i, such that $u_i = \frac{\partial \Psi_i}{\partial y}$ and $v_i = -\frac{\partial \Psi_i}{\partial x}$. We now assume a sinusoidal disturbance and write

$$\Psi_i = \psi_i(y)e^{ik(x-ct)} + c.c. \tag{20}$$

where $c.c.$ denotes complex conjugate. $\psi(y)$ is the complex amplitude, k is the dimensionless real wave number and $c = c_R + ic_I$ is the dimensionless complex wave speed. The real part c_R is the phase velocity of the wave, while kc_I is its growth rate. More precisely, the flow is unstable if $c_I > 0$, stable if $c_I < 0$ and neutrally stable when $c_I = 0$. Substitution of (20) into (16) and (17) yields upon elimination of p_i by taking the curl, the following two Orr-Sommerfeld equations for the two fluids

$$\big(D^2 - k^2\big)^2\psi_1 = i\frac{k\gamma R_2}{m}\Big[(U_1 - c)(D^2 - k^2) - D^2U_1\Big]\psi_1 \tag{21}$$

for the upper phase $0 < y < 1$, and

$$\big(D^2 - k^2\big)^2\psi_2 = ikR_2\Big[(U_2 - c)(D^2 - k^2) - D^2U_2\Big]\psi_2 \tag{22}$$

for the lower phase $-1 < y < 0$. The conditions at the interface are the continuity of the velocity components and the balance of the stress components. Formally speaking, these conditions must be evaluated at $y = \eta(x,t)$, the location of the interface in the disturbed situation, and not at the originally interface y = 0. This modification is taken into account by means of a Taylor expansion in η around y = 0. The interface conditions then read $\eta = \frac{\psi_1(0)}{c-U_1(0)} e^{ik(x-ct)}$. Finally we can rewrite the boundary conditions in terms of ψ_i, k, c and R_i correcting to the leading order in η, and the details of the derivation are presented in appendix B.

at $y = 1$: $\psi_1 = D\psi_1 = 0$

at $y = -1$: $\psi_2 = D\psi_2 = 0$

at the interface $y = 0$:

- $\psi_1 = \psi_2$
- $\big(D\psi_1 - D\psi_2\big) + \big(DU_1 - DU_2\big)\frac{\psi_1}{c-U_1} = 0$
- $\big(D^2 + k^2\big)\big(m\psi_1 - \psi_2\big) + \big(mD^2U_1 - D^2U_2\big)\frac{\psi_1}{c-U_1} = 0$
- $m\big(D^3 - 3k^2D\big)\psi_1 - \big(D^3 - 3k^2D\big)\psi_2 + ik\gamma R_2\big[(c-U_1)D + DU_1\big]\psi_1 - ikR_2\big[(c-U_2)D + DU_2\big]\psi_2 + ikR_2\Big[(1-\gamma)\frac{\cos\theta}{F^2} + k^2S\Big]\frac{\psi_1}{c-U_1} = 0$

3 Linear stability analysis

Systems (21) and (22) with corresponding boundary conditions have an infinite number of eigenvalues and associated eigenfunctions. Since the real part of the temporal growth rate in (20) is e^{-ikc}; $c = c_R + ic_I$; the eigenvalue which has largest imaginary part is most dangerous in a linear instability analysis. In order to determine the complex eigenvalue c, the eigenfunctions ψ_i are approximated by the Galerkin truncation of the Chebyshev polynomial of first kind. Then the eigenvalue problem is discretized and formed a generalized matrix eigenvalue problem (see details in Appendix C)

$$\mathbf{A}\vec{x} = c\mathbf{B}\vec{x} \tag{23}$$

where $\vec{x} = (\psi_1, \psi_2)^\top$. The matrices $\mathbf{A}$ and $\mathbf{B}$ are singular because some of the boundary and interface conditions do not contain the eigenvalue c. This singularity is handled by deflating the infinite eigenvalues using the standard QZ-algorithm. Grid convergence has been checked by varying number of collocation points, and in most calculations 100 collocation points are used. Furthermore, the implemented algorithm has been validated by against the tow-layer plane Poiseuille flow problem in [6] which is also presented in Appendix C. Excellent agreement was found in all cases. The linear stability study will be discussed in the following parts of the section. For simplicity, we assume that two fluid have the same dynamic viscosity from now on.

3.1 Stokes flow

For an extreme example, it is interesting to study the inertialess stability and let the Reynolds number be zero. Thus in the absence of the surface tension the linear equations, i.e., the Orr-Sommerfeld equations can be reduced to

$$\begin{cases} \left(D^2-k^2\right)^2\psi_1=0, & 0<y<1 \\ \left(D^2-k^2\right)^2\psi_2=0, & -1<y<0 \\ \psi_1(1)=D\psi_1(1)=0, & \text{at } y=1 \\ \psi_2(-1)=D\psi_2(-1)=0, & \text{at } y=-1 \\ \psi_1=\psi_2, \quad D\psi_1=D\psi_2, & \text{at } y=0 \\ \left(D^2\psi_1-D^2\psi_2\right)c+16\psi_1=0, & \text{at } y=0 \\ \left(D^3\psi_1-D^3\psi_2\right)c+16ik\cot\theta\psi_1=0, & \text{at } y=0 \end{cases} \tag{24}$$

It is easy to find the general solution for Stokes flow

$$\psi_1 = a_1e^{ky}+b_1e^{-ky}+c_1ye^{ky}+d_1ye^{-ky} \tag{25}$$

$$\psi_2 = a_2e^{ky}+b_2e^{-ky}+c_2ye^{ky}+d_2ye^{-ky} \tag{26}$$

From the boundary conditions, we once more obtain a secular equation by setting the determinant of the coefficients of a_i, b_i, c_i and d_i to zero:

$$\begin{vmatrix} e^k & e^{-k} & e^k & e^{-k} & 0 & 0 & 0 & 0 \\ ke^k & -ke^{-k} & (1+k)e^k & (1-k)e^{-k} & 0 & 0 & 0 & 0 \\ 0 & 0 & 0 & 0 & e^{-k} & e^k & -e^{-k} & -e^k \\ 0 & 0 & 0 & 0 & ke^{-k} & -ke^k & (1-k)e^{-k} & (1+k)e^k \\ 1 & 1 & 0 & 0 & -1 & -1 & 0 & 0 \\ k & -k & 1 & 1 & -k & k & -1 & -1 \\ k^2c+16 & k^2c+16 & 2kc & -2kc & -k^2c & -k^2c & -2kc & 2kc \\ k^3c+iNk & -k^3c+iNk & 3k^2c & 3k^2c & -k^3c & k^3c & -3k^2c & -3k^2c \end{vmatrix} = 0$$

where we define $N \triangleq 16\cot\theta$. Direct computation yields the determinant

$$c = iN\frac{4k^2\sinh(2k)+4k\cosh(2k)+2\sinh(2k)-\sinh(4k)-4k-8k^3}{4k^2\cosh(4k)-4k^2-32k^4} \tag{27}$$

Numerical computation shows that the above expression can not be positive for all wave number k, which implies Stokes flow is always stable for any tilt angle $< \frac{\pi}{2}$. Typical relationship between the wave number k and the growth rate is plotted when the tilt angle is $\frac{\pi}{3}$, together with numerical results using the Chebyshev-tau method and the asymptotic expansion as k is small in Fig.2.

3.2 General case

In this part, we consider the effects of density ratio, tilt angle, Reynolds number and surface tension on the linear stability problem for the general Orr-Sommerfeld equation. Fig.3 shows a typical profile of the unstable eigenmode and its velocity field.

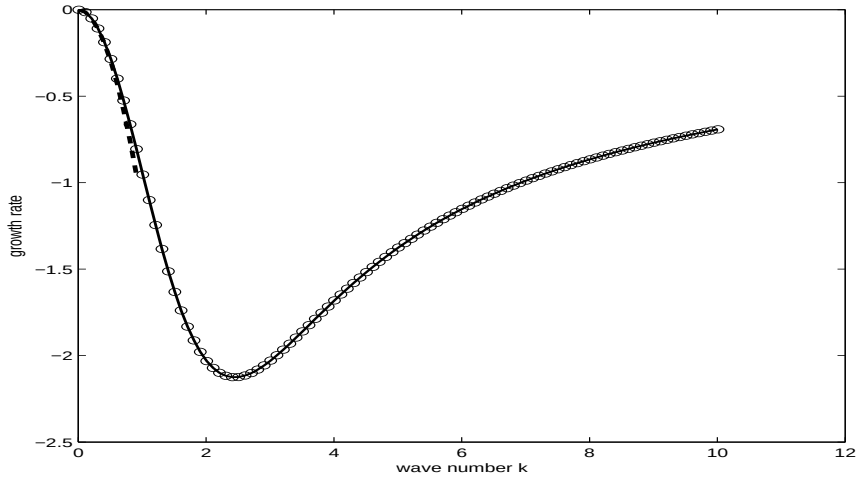

Figure 2: Growth rate versus wave number for Stokes wave at $\theta = \frac{\pi}{3}$. Solid line is the theoretical prediction, the circle ones are numerical results, and the dash line is the asymptotic expansion when wave number k is fairly small.

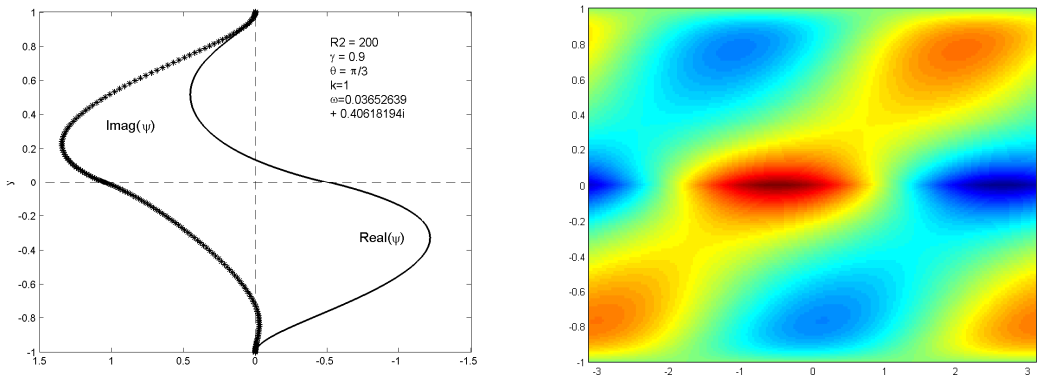

Figure 3: Typical steam function of the unstable eigenvalue and its velocity vector field. On the right hand side, the red color means the right direction vector, while the blue color represents the left direction vector.

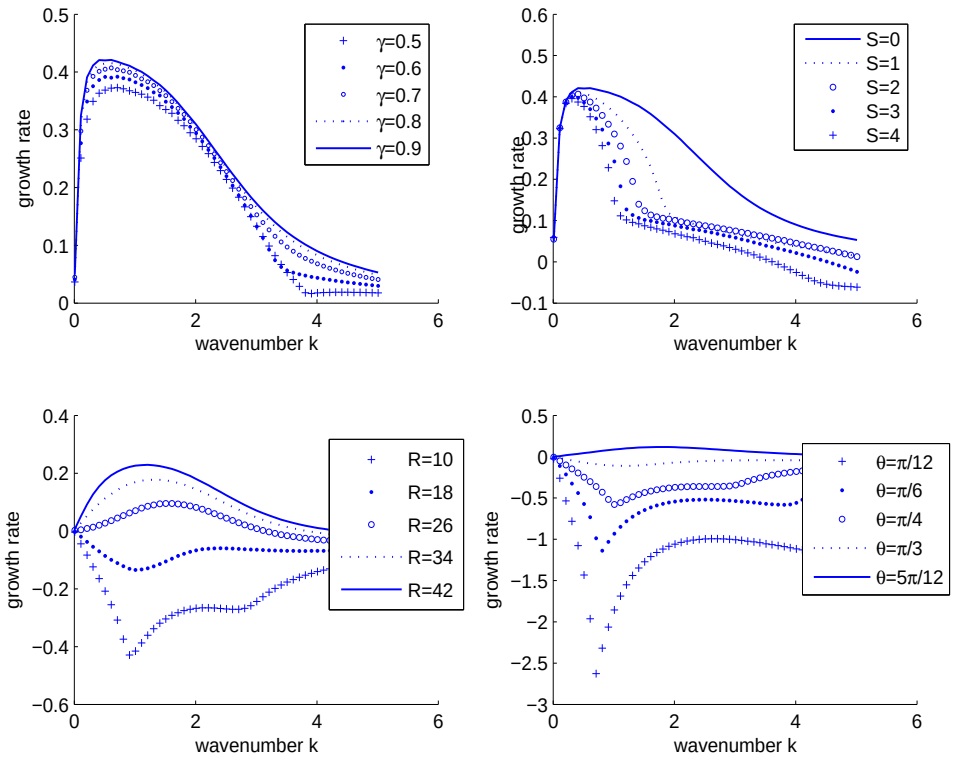

Figure 4: Growth rate versus wave number k. Upper left: $R_2 = 200, S = 0, \theta = \pi/3$; Upper right: $R_2 = 200, \gamma = 0.9, \theta = \pi/3$; Lower left: $\gamma = 0.9, \theta = \pi/3, S = 0$; Lower right: $R_2/\sin\theta = 10, \gamma = 0.9, S = 0$.

In Fig.4, the effect density ratio, surface tension, Reynolds number and tilt angle are plotted respectively. The upper left picture shows that the density ratio has little effect on the stability property. We check the density ratio from 0.5 to 0.9, the basic behavior of the growth rate curve does not change much. The upper right picture shows that the surface tension would stabilize the system a little bit but not very significant especially when the wave number k is very small, that is because for long wave approximation, the surface tension is of order k^4 in the Fourier space (See more details in the next section). In the lower-half part of Fig.4, two plots show the Reynolds number and the tilt angle are two main factors in stability analysis. Both of them have destabilizing effect. It is worth mentioning that Reynolds number is not a good parameter in the lab, since

$$R_2 = \frac{\rho_2 HU}{\mu_2} = \frac{\rho_2^2 H g'}{\mu_2^2(1 + m^2 + 14m)} \sin\theta \tag{28}$$

It is obvious that $R_2/\sin\theta$ is an appropriate parameter for studying the effect of tilt angle. In the lower right of Fig.4, we fix $R_2/\sin\theta = 10$ instead of fixing the Reynolds number.

Fig.5 plots the relationship between the tilt angle θ and $R_2/\sin\theta$, the parameter used to replace the Reynolds number, for generating the instability. It shows that when $R_2/\sin\theta$ is rather small or big, the curve is quite smooth, but in between the points are a little bit messy due to the modes crossings.

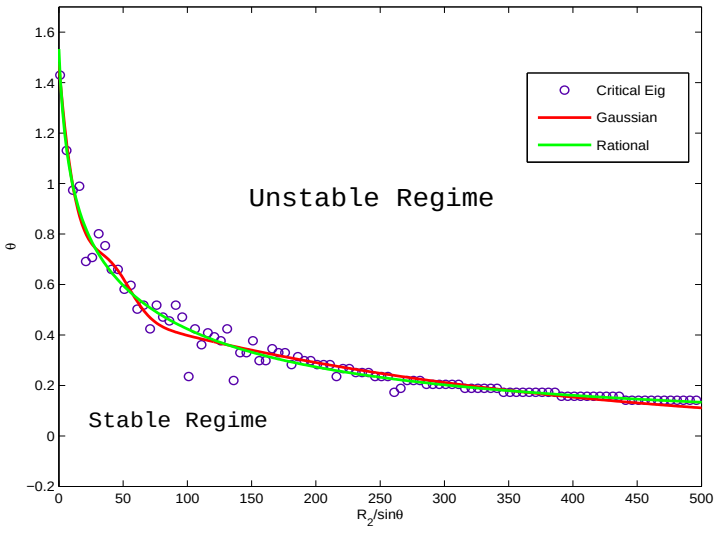

Figure 5: Curve for separating stable region and unstable region. The circle ones are the numerical results of Orr-Sommerfeld systems, two solid lines are the fitting curves using different functions: rational function (green) and gaussian function (red).

4 Weakly nonlinear model for long wave perturbation

In this section, we use multi-scale method to establish a weakly nonlinear model for the interface evolution in long wave perturbation setting. The ansatz for slow-varying small amplitude perturbation is

$$\eta = \epsilon A(X,T) \tag{29}$$
$$\Psi_1 = \epsilon\Psi_{10}(X,Y,T) + \epsilon^2\Psi_{11}(X,Y,T) + O(\epsilon^3) \tag{30}$$
$$\Psi_2 = \epsilon\Psi_{20}(X,Y,T) + \epsilon^2\Psi_{21}(X,Y,T) + O(\epsilon^3) \tag{31}$$

with $X = \epsilon x$, $Y = \epsilon y$ and $T = \epsilon^2 t$ where ϵ is a small parameter. Due to the expression of η, it is convenient to rewrite Ψ_{10} and Ψ_{20} as

$$\Psi_{10}(X,Y,T) = A(X,T)\phi_0(Y)$$
$$\Psi_{20}(X,Y,T) = A(X,T)\chi_0(Y)$$

Substitution of the above expressions into perturbed full Navier-Stokes equations and corresponding boundary conditions, taking $m = 1$ and collecting terms of first order of ϵ, yield

$$\begin{cases} D^4\phi_0 = D^4\chi_0 = 0, & \text{governing equations} \\ \phi_0(1) = D\phi_0(1) = 0, & \text{no-slip conditions at } y = 1 \\ \chi_0(-1) = D\chi_0(-1) = 0, & \text{no-slip conditions at } y = -1 \\ \phi_0 = \chi_0, \quad D\phi_0 = D\chi_0, & \text{at the interface } y = 0 \\ D^2\phi_0 - D^2\chi_0 + 16 = 0, & \text{tangential stress at } y = 0 \\ D^3\phi_0 = D^3\chi_0, & \text{normal stress at } y = 0 \end{cases} \tag{32}$$

After direct calculations, the solutions of this ODE system are

$$\begin{cases} \phi_0 = 2y^3 - 4y^2 + 2y \\ \chi_0 = 2y^3 + 4y^2 + 2y \end{cases} \tag{33}$$

Then we turn to the second order of the expansion. The second order approximation is obtained by collecting terms of order ϵ^2, which yields the following inhomogeneous ordinary differential system

$$\begin{cases} D^4\Psi_{11} = R_1 A_X (U_1 D^2 - D^2 U_1)\phi_0, & \text{governing equations} \\ D^4\Psi_{21} = R_2 A_X (U_2 D^2 - D^2 U_2)\chi_0, & \text{governing equations} \\ \Psi_{11}(1) = D\Psi_{11}(1) = 0, & \text{no-slip conditions at } y = 1 \\ \Psi_{21}(-1) = D\Psi_{21}(-1) = 0, & \text{no-slip conditions at } y = -1 \\ \Psi_{11} = \Psi_{21}, & \text{at the interface } y = 0 \\ D\Psi_{11} - D\Psi_{21} = 8A^2, & \text{at the interface } y = 0 \\ D^2\Psi_{11} = D^2\Psi_{21}, & \text{tangential stress at } y = 0 \\ D^3\Psi_{11} - D^3\Psi_{21} + (16A_X \cot\theta - S\epsilon^2 A_{XXX}) = 0, & \text{normal stress at } y = 0 \end{cases} \tag{34}$$

Here the surface tension is supposed to be very large between oil and water interface, i.e., $S = O(1/\epsilon^2)$. Observing the governing equations and boundary conditions carefully, we can assume that

$$\Psi_{11} = m_1(Y)A_X + m_2(Y)A^2 + m_3(Y)A_{XXX} \tag{35}$$

$$\Psi_{21} = n_1(Y)A_X + n_2(Y)A^2 + n_3(Y)A_{XXX} \tag{36}$$

After a tedious computation, we substitute the solution of (34) into the kinematic boundary condition and collect the $O(\epsilon^3)$ terms, then obtain

$$A_T + a_1 A A_X + a_2 A_{XX} + a_3 A_{XXXX} = 0 \tag{37}$$

with

$$\begin{aligned} a_1 &= \big(2D^2U_1 + 2D\phi_0 + 2m_2\big)(0) = 8 \\ a_2 &= m_1(0) = \frac{1}{70}(R_1 + R_2) - \frac{2}{3}\cot\theta \\ a_3 &= m_3(0) = \frac{S\epsilon^2}{24} \end{aligned}$$

This is a typical Kuramoto-Sivashinsky equation when a_2 is big than 0, and its steady solution, properties and globally well-posedness have been studied. When $a_2 < 0$, it becomes diffusion equation which is globally well-posed. If neglecting the nonlinear term, using standard Fourier analysis, the dispersion relation reads

$$c = i\big(a_2 k - a_3 k^3\big) \tag{38}$$

substitution of the dispersion relation into the Fourier mode $e^{ik(X-cT)}$, one obtains the growth rate equals $e^{(a_2k^2 - a_3k^4)T}$. It shows that the surface tension has stabilizing effect on

the system. If neglecting the surface tension term, the sign of a_2 determines the stability property of the system, which gives a sufficient condition between Reynolds number and tilt angle for generating the instability:

$$\cot\theta < \frac{3}{140}\big(R_1 + R_2\big) \tag{39}$$

5 Conclusion

By the end of the project, I hoped to have an answer, either analytic or numerical, for the stability of the two-layer viscous fluid in an inclined closed tube subject to small perturbations and find the effects of surface tension, tilt angle, Reynolds number, density ratio and wave number in triggering the instability. For the linear stability analysis, Chebyshev-tau method is applied to two-layer Orr-Sommerfeld equations. Tilt angle and Reynolds number both have the effect to destabilize the system, while the surface tension stabilize it. Stokes flow is studied as an extreme example showing that it is stable for any tilt angle. Except this, for any Reynolds number, one can find a tilt angle to generate the instability. Furthermore, a weakly nonlinear model equation for long wave perturbation is derived and found to be Kuramoto-Sivashinsky type. If neglecting the surface tension effects, it offers a sufficient condition on Reynolds number and the tilt angle for generating linear instability, which totally depends on the coefficient of A_{XX} term.

6 Acknowledgements

I would like to take the opportunity to thank staff in 2011 GFD summer school, especially the two main lecturers Fabian and Rich and the organizers Norman, Phil and Janet. Also, I'd like to thank Jack, Olivier, Fabian, Leslie, Joe and Phil for their guidance and advice throughout the summer. I would like to thank George for his coaching and enthusiasm through the summer's softball practices and games. Last but not least, I'd like to thank all the fellows for the late nights in Walsh Cottage, fantastic dinners, trips to the beach, and more.

7 Appendix A. derivation of base shear flow

In this section the basic unperturbed flow pattern is obtained. The unperturbed flow is parallel to the x-axis and the velocity is a function of y only. Both of the fluids have the same depth H. The Navier-Stokes equations that govern the basic flow are

$$-\frac{1}{\rho_i}\frac{\partial \widetilde{P}_i}{\partial x} + g\sin\theta + \frac{\mu_i}{\rho_i}\frac{\partial^2 \widetilde{u}_i}{\partial y^2} = 0 \tag{40}$$

$$-\frac{1}{\rho_i}\frac{\partial \widetilde{P}_i}{\partial y} - g\cos\theta = 0 \tag{41}$$

From equation (41), one obtains $\widetilde{P}_i = -\rho_i g\cos\theta y + \big(\text{function of x}\big)$. Since $\frac{\partial^2 \widetilde{u}_i}{\partial y^2}$ is a function of y only, from (40) it is clear that $\frac{\partial \widetilde{P}_1}{\partial x}$ and $\frac{\partial \widetilde{P}_2}{\partial x}$ are both constants. Then the solutions for

$\widetilde{u}_i$ take the form

$$\widetilde{u}_1 = (-\frac{\rho_1 g}{\mu_1}\sin\theta + c_1)\frac{y^2}{2} + a_1 y + b_1 \tag{42}$$

$$\widetilde{u}_2 = (-\frac{\rho_2 g}{\mu_2}\sin\theta + c_2)\frac{y^2}{2} + a_2 y + b_2 \tag{43}$$

where a_i, b_i and c_i are all constants need to be determined by the boundary conditions. Using the boundary conditions at the interface $y = 0$: $\widetilde{u}_1 = \widetilde{u}_2$, $\mu_1\frac{\partial\widetilde{u}_1}{\partial y} = \mu_2\frac{\partial\widetilde{u}_2}{\partial y}$ and $\widetilde{P}_1 = \widetilde{P}_2$, one obtains $a_2 = ma_1$, $b_1 = b_2$ and $c_2 = mc_1$ respectively, where $m = \frac{\mu_1}{\mu_2}$ is the dynamic viscosity ratio. For simplicity, let's denote $c_1 \triangleq c$, $a_1 \triangleq a$ and $b_1 \triangleq b$. On the other hand, because the tube is closed, then there is no flux across any place $x = constant$, which implies

$$\begin{aligned} &\int_{-H}^{0}\widetilde{u}_2 dy + \int_{0}^{H}\widetilde{u}_1 dy = 0 \\ \Longrightarrow\quad & b = \frac{H^2}{12}\Big[\Big(\frac{\gamma}{m}+1\Big)\frac{\rho_2}{\mu_2}g\sin\theta - (1+m)c\Big] - \frac{H}{4}\big(1-m\big)a \end{aligned} \tag{44}$$

Finally, applying the no-slip boundary conditions at the fixed walls, one obtains

$$\Big(-\frac{\gamma\rho_2 g\sin\theta}{m\mu_2} + c\Big)\frac{H^2}{2} + aH + \frac{H^2}{12}\Big[\Big(\frac{\gamma}{m}+1\Big)\frac{\rho_2 g\sin\theta}{\mu_2} - (1+m)c\Big] - \frac{H}{4}\big(1-m\big)a = 0$$

$$\Big(-\frac{\rho_2 g\sin\theta}{\mu_2} + mc\Big)\frac{H^2}{2} - amH + \frac{H^2}{12}\Big[\Big(\frac{\gamma}{m}+1\Big)\frac{\rho_2 g\sin\theta}{\mu_2} - (1+m)c\Big] - \frac{H}{4}\big(1-m\big)a = 0$$

Therefore, we solve the linear system for a and c

$$a = \frac{4(\gamma-1)}{1+m^2+14m}\frac{\rho_2}{\mu_2}gH\sin\theta \tag{45}$$

$$b = \frac{(1-m)(1-\gamma)}{1+m^2+14m}\frac{\rho_2}{\mu_2}\frac{gH^2\sin\theta}{2} \tag{46}$$

$$c = \frac{7m+\gamma+m^2+7m\gamma}{m(1+m^2+14m)}\frac{\rho_2}{\mu_2}g\sin\theta \tag{47}$$

Finally, we get the base shear flow

$$\widetilde{u}_1 = \frac{(1-\gamma)g}{1+m^2+14m}\frac{\rho_2}{\mu_2}\sin\theta\Big[\frac{7+m}{2}y^2 - 4Hy + \frac{1-m}{2}H^2\Big] \tag{48}$$

$$\widetilde{u}_2 = \frac{(1-\gamma)g}{1+m^2+14m}\frac{\rho_2}{\mu_2}\sin\theta\Big[-\frac{7m+1}{2}y^2 - 4mHy + \frac{1-m}{2}H^2\Big] \tag{49}$$

8 Appendix B. boundary conditions on the interface

In this part, we give the details of the derivation of the stress continuity on the interface in terms of the stream functions. First of all, we know

$$u_i = \frac{\partial\Psi_i}{\partial y} = D\psi_i e^{ik(x-ct)} \tag{50}$$

$$v_i = -\frac{\partial\Psi_i}{\partial x} = -ik\psi_i e^{ik(x-ct)} \tag{51}$$

Furthermore, we assume the interface is designated as $\eta(x,t) = \hat{\eta}e^{ik(x-ct)}$. Following the notation in section 2.1, the kinematic boundary condition $\eta_t = v_1' - \eta_x u_1'$ can be linearized as $\eta_t = v_1 - \eta_x U_1$, then one obtains

$$-ikc\hat{\eta} = -ik\psi_1 - ik\hat{\eta}U_1 \Longrightarrow \hat{\eta} = \frac{\psi_1(0)}{c - U_1(0)} \tag{52}$$

For the continuity of velocity at the interface, $v_1' = v_2'$ is trivial, while $u_1' = u_2'$ results in

$$\begin{aligned} & U_1 + \eta DU_1 + u_1 + \cdots = U_2 + \eta DU_2 + u_2 + \cdots \\ \Longrightarrow \quad & \big(D\psi_1 - D\psi_2\big) + \big(DU_1 - DU_2\big)\frac{\psi_1(0)}{c - U_1(0)} = 0 \end{aligned} \tag{53}$$

Then for the tangential stress, taking expansion about $y = 0$, one obtains

$$\begin{aligned} & m\Big(\frac{\partial v_1'}{\partial x} + \frac{\partial u_1'}{\partial y}\Big) = \frac{\partial v_2'}{\partial x} + \frac{\partial u_2'}{\partial y} \\ \Longrightarrow \quad & m\Big[\frac{\partial v_1}{\partial x} + \frac{\partial(u_1 + U_1 + DU_1\eta + \cdots)}{\partial y}\Big] = \frac{\partial v_2}{\partial x} + \frac{\partial(u_2 + U_2 + DU_2\eta + \cdots)}{\partial y} \\ \Longrightarrow \quad & \big(D^2 + k^2\big)\big(m\psi_1 - \psi_2\big) + \big(mD^2U_1 - D^2U_2\big)\hat{\eta} = 0 \\ \Longrightarrow \quad & \big(D^2 + k^2\big)\big(m\psi_1 - \psi_2\big) + \big(mD^2U_1 - D^2U_2\big)\frac{\psi_1(0)}{\omega - U_1(0)} = 0 \end{aligned} \tag{54}$$

For later use, we point out the following formula $\hat{\eta} = \frac{\psi_1(0)}{c-U_1(0)} = -\frac{(D^2+k^2)(m\psi_1-\psi_2)}{mD^2U_1-D^2U_2}$. In order to obtain the normal stress formula, we need the expression of the presure. Assuming $p_i = \hat{p}_i e^{ik(x-ct)}$, using equation (8), we can get

$$\hat{p}_i = \frac{1}{ikR_i}\big(D^3\psi_i - k^2 D\psi_i\big) + cD\psi_i + DU_i\psi_i - U_i D\psi_i \tag{55}$$

Now we can rewrite the normal stress boundary condition in a suitable form,

$$\begin{aligned} & \big(-P_2' + \frac{2}{R_2}\frac{\partial v_2'}{\partial y}\big) - \gamma\big(-P_1' + \frac{2}{R_1}\frac{\partial v_1'}{\partial y}\big) - S\frac{\partial^2\eta}{\partial x^2} = 0 \\ \Longrightarrow \quad & \big(-p_2 - DP_2'\eta + \frac{2}{R_2}\frac{\partial v_2}{\partial y} - \cdots\big) - \gamma\big(-p_1 - DP_1'\eta + \frac{2}{R_1}\frac{\partial v_1}{\partial y} - \cdots\big) - S\frac{\partial^2\eta}{\partial x^2} = 0 \\ \Longrightarrow \quad & \big(\gamma\hat{p}_1 - \hat{p}_2\big) + \frac{2ik}{R_2}\big(mD\psi_1 - D\psi_2\big) + \Big[(1-\gamma)\frac{\cos\theta}{F^2} + k^2 S\Big]\hat{\eta} = 0 \\ \Longrightarrow \quad & m\big(D^3 - 3k^2D\big)\psi_1 - \big(D^3 - 3k^2D\big)\psi_2 + ik\gamma R_2\big[(c-U_1)D + DU_1\big]\psi_1 \\ & -ikR_2\big[(c-U_2)D + DU_2\big]\psi_2 + ikR_2\Big[(1-\gamma)\frac{\cos\theta}{F^2} + k^2 S\Big]\frac{\psi_1}{c-U_1} = 0 \end{aligned} \tag{56}$$

For numerical purpose, we need rewrite the normal stress in the following way

$$\begin{aligned} & m\big(D^3 - 3k^2D\big)\psi_1 - \big(D^3 - 3k^2D\big)\psi_2 + ik\gamma R_2\big[(c-U_1)D + DU_1\big]\psi_1 - ikR_2\big[(c \\ & -U_2)D + DU_2\big]\psi_2 - ikR_2\Big[(1-\gamma)\frac{\cos\theta}{F^2} + k^2 S\Big]\frac{(D^2+k^2)(m\psi_1 - \psi_2)}{mD^2U_1 - D^2U_2} = 0 \end{aligned} \tag{57}$$

9 Appendix C. numerical method

Step 1. Coordinate transformation

Chebyshev polynomials are orthogonal on the interval $[-1,1]$. In order to use the Chebyshev-tau QZ-algorithm to solve the generalized eigenvalue problem, we need transform the Orr-Sommerfeld equations on either of the intervals $[-1,0]$ and $[0,1]$ to the interval $[-1,1]$ by a change of the independent variable y. This is easily achieved by means of the linear transformations

$$\begin{cases} z = 2y - 1 & 0 \leqslant y \leqslant 1 \\ z = -2y - 1 & -1 \leqslant y \leqslant 0 \end{cases} \tag{58}$$

It is noted that $z = -1$ becomes the interface in both cases. Then the Orr-Sommerfeld equations in new coordinates become

$$\Big(4D^2 - k^2\Big)^2 \psi_i - ikR_i\Big[U_i\big(4D^2 - k^2\big) - U_i''\Big]\psi_i = \Big[- ikR_i\big(4D^2 - k^2\big)\psi_i\Big]c \tag{59}$$

Here D presents the derivative with respect to the new variable z and $'$ means the derivative w.r.t the old variable y. Furthermore, the rigid wall boundary condition in the new coordinates become

$$\psi_1(1) = D\psi_1(1) = \psi_2(1) = D\psi_2(1) = 0 \tag{60}$$

The interface boundary conditions are, on $z = -1$

$$\psi_1 - \psi_2 = 0 \tag{61}$$

$$\big(2U_1 D - U_1' + U_2'\big)\psi_1 + 2U_1 D\psi_2 = \big(2D\psi_1 + 2D\psi_2\big)c \tag{62}$$

$$\big(4mD^2 + mk^2 - mU_1'' + U_2''\big)\psi_1 - \big(4D^2 + k^2\big)\psi_2 = \big(4D^2 + k^2\big)\big(m\psi_1 - \psi_2\big)c \tag{63}$$

$$\begin{aligned} &m\big(8D^3 - 6k^2 D\big)\psi_1 + \big(8D^3 - 6k^2 D\big)\psi_2 + i\Big[k\gamma R_2\big(U_1' - 2U_1 D\big)\psi_1 \\ &-kR_2\big(2U_2 D + U_2'\big)\psi_2 - k\Big(\cot\theta + \frac{k^2 T}{\sin\theta}\Big)\big(4D^2 + k^2\big)\big(m\psi_1 - \psi_2\big)\Big] \\ &= -i\Big(2k\gamma R_2 D\psi_1 + 2kR_2 D\psi_2\Big)c \end{aligned} \tag{64}$$

where $T \triangleq \frac{\sigma}{\rho_2 g' H^2}$ is a new parameter.

Step 2. Galerkin truncation and point collocation

Approximating the eigenfunction ψ_1 and ψ_2 by the truncated Chebyshev expansions

$$\psi_1(z) = \sum_{n=0}^{N} a_n T_n(z), \qquad \psi_2 = \sum_{n=0}^{N} b_n T_n(z) \tag{65}$$

where $T_n(z)$ is the nth order first-kind Chebyshev polynomial. The high order derivatives of the eigenfunction can be found by differentiating the Chebyshev polynomial. Our goal is to determine the coefficients a_n, b_n and the eigenvalue ω. For this purpose, we need

$2(N+1)$ conditions. We collocate the Galerkin truncation at the extrema of the Chebyshev polynomial

$$z = \cos\Big(\frac{j\pi}{M}\Big), \qquad j = 1 \cdots M-1 \tag{66}$$

We pick $M = N-2$, thus if we evluate the Orr-Sommerfeld equation at these extrema points, we obtain $2N-6$ linear algbraic equations. The other eight conditions come from the corresponding boundary conditions mentioned in step 1. Therefore we complete our system.

Step 3. Generalized eigenvalue problem

We denote

$$A_R \triangleq \begin{pmatrix} 16D^4 - 8k^2D^2 + k^4 & 0 \\ BC1 \sim 4 & BC1 \sim 4 \\ 0 & 16D^4 - 8k^2D^2 + k^4 \\ BC5 \sim 8 & BC5 \sim 8 \end{pmatrix} \tag{67}$$

$$A_I \triangleq \begin{pmatrix} -kR_1\big[U_1(4D^2 - k^2) - U_1''\big] & 0 \\ BC1 \sim 4 & BC1 \sim 4 \\ 0 & -kR_2\big[U_2(4D^2 - k^2) - U_2''\big] \\ BC5 \sim 8 & BC5 \sim 8 \end{pmatrix} \tag{68}$$

$$B_R \triangleq \begin{pmatrix} 0 & 0 \\ BC1 \sim 4 & BC1 \sim 4 \\ 0 & 0 \\ BC5 \sim 8 & BC5 \sim 8 \end{pmatrix} \tag{69}$$

and

$$B_R \triangleq \begin{pmatrix} -kR_1(4D^2 - k^2) & 0 \\ BC1 \sim 4 & BC1 \sim 4 \\ 0 & -kR_2(4D^2 - k^2) \\ BC5 \sim 8 & BC5 \sim 8 \end{pmatrix} \tag{70}$$

where $BC1 \sim 4$ represents the boundary conditions (60), while $BC5 \sim 8$ the boundary conditions (61)-(64). We therefore can write the system of equations as a generalized eigenvalue problem

$$\Big[A_R + iA_I\Big]\mathbf{x} = c\Big[B_R + iB_I\Big]\mathbf{x} \tag{71}$$

where $\mathbf{x} = (a_0, \cdots, a_N, b_0, \cdots, b_N)^\top$. Using QZ-algorithm in MATLAB, it is easy to obtain the eigenvalues and corresponding eigenvectors.

Step 4. Validation

Two examples are presented here for the purpose of validation. The first example is the

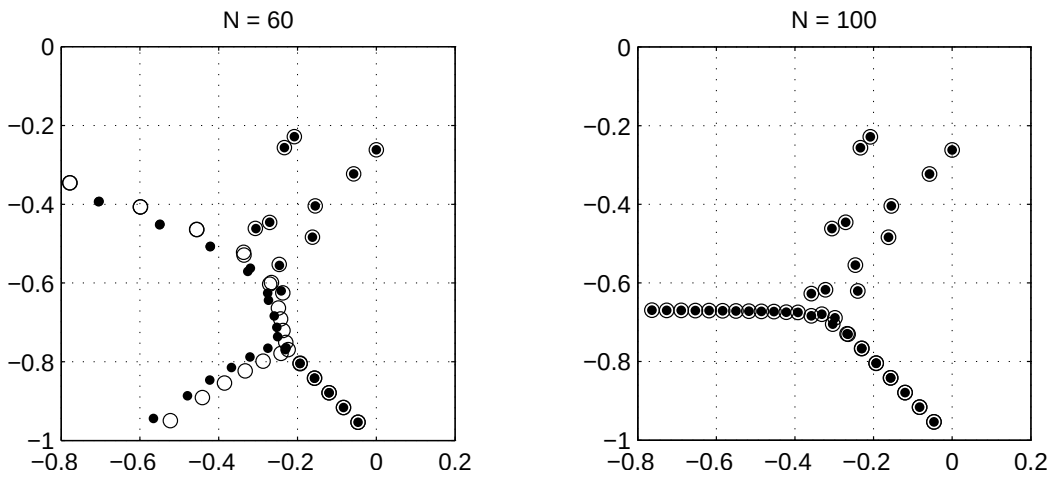

Figure 6: Eigenvalues for plane Poiseuille at Raynolds number 5772. The dots are for the general Chebyshev method and the empty circles are for Chebyshev-tau method. Left picture uses 60 collocation points and the right one uses 100 points

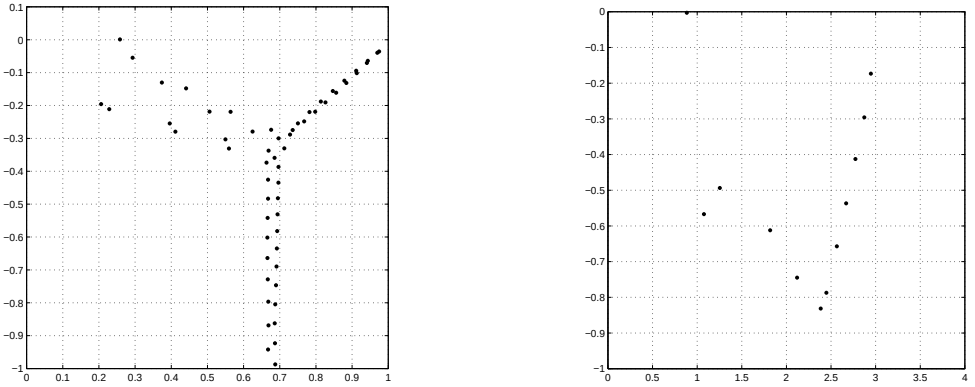

Figure 7: Eigenvalues for two-layer plane Poiseuille flow. Left: $Re = 10^4$, $a = 1$, $m = 2$, $n = 1.2$, $u_n = 0$. Right: $Re = 25$, $a = 1$, $m = 2$, $n = 10$, $u_n = 3$

one-layer plane Poiseuille flow at Reynolds number 5772. The resulting eigenvalues using general Chebyshev method presented in Page 150 of [17] and Chebyshev-tau method are both plotted in Fig.6. It is clear that when collocation points are increased to 100 points, the results for two methods coincide with each other perfectly. For our linear problem in the paper, we use 100 points for all numerical experiments. Another numerical experiment is carried out for the two-layer Poiseuille flow and compared with the results in [6]. In Fig.7 the plots are the eigenvalues for different height ratios and Reynolds numbers. The results agree with the Pic.7 and Pic.9 of paper [6] very well. And numbers in the following table show the comparison of the leading eigenmodes between the left hand-side of Fig.7 and Pic.7 in [6].

Model type	Our codes	Dongarra's results
interface	0.00172758052977	0.00179188368
shear	0.00087962166886	0.0008778915187

References

[1] A.P. Bassom, M.G. Blyth, D.T. Papageorgiou, Nonlinear development of two-layer Couette-Poiseuille flow in the presence of surfactant, Phys. Fluids, 22(10), 2010.

[2] P.A.M. Boomkamp, B.J. Boersma, R.H.M. Miesen, G.V. Beijnon, A chebyshev collocation method for solving two-phase flow stability problems, J. Comp. Phys., 132, 191-200, 1997.

[3] A. Bague, D. Fuster, S. Popinet, R. Scardovelli, S. Zaleski, Instability growth rate of two-phase mixing layer from a linear eigenvalue problem and an initial-value problem, Phys. Fluids, 22(1), 2010.

[4] C. Cenedese, J.A. Whitehead, T.A. Ascarelli, M. Ohiwa, A dense current flowing down a sloping bottom in a rotating fluid, J. Phys. Oceanogr., 34, 188-203, 2002.

[5] A. Defina, S. Lanzoni, F.M. Susin, Stability of a stratified viscous shear flow in a title tube, Phys. Fluids, 11(2), 1998.

[6] J.J. Dongarra, B. Straughan, D.W. Walker, Chebyshev tau-QZ algorithm methods for calculating spectra of hydrodynamic stability problems, J. Appl. Nume. Math., 22(4), 1996.

[7] H. Fouli, D.Z. Zhu, Interfacial waves in two-layer exchange flows downslope of a bottom sill, J. Fluid Mech., 680, 194-224, 2011.

[8] A.P. Hooper, W.G.C. Boyd, shear-flow instability at the interface between two viscous fluids, J. Fluid Mech., 128, 507-528, 1983.

[9] A.P. Hooper, R. Grimshaw, Nonlinear instability at the interface between two viscous fluids, Phys. Fluids, 28(1), 1985.

[10] T.W. Kao, Stability of two-layer viscous stratified flow down an inclined plane, Phys. Fluids, 8(5), 1965.

[11] H. Kim, J.C. Padrino, D.D. Joseph, Viscous effects on Kelvin-Helmholtz instability in a channel, J. Fluid Mech., 680, 398-416, 2011.

[12] S. Mählmann, D.T. Papageorgiou, Interfacial instability in electrified plane Couette flow, J. Fluid Mech., 666, 155-188, 2011.

[13] O. Marchal, J.A. Whitehead, Penetration of a salinity front into the ocean interior: laboratory experiments and a simple theory, to appear in J. Phys. Oceanogr., 2011.

[14] D.I. Meiron, G.R. Baker, S.A. Orszaga, Analytic structure of vortex sheet dynamics. Part 1. Kelvin-Helmholtz instability, J. Fluid Mech., 114, 283-298, 1982.

[15] M.E. Negretti, S.A. Socolofsky, G.H. Jirka, Linear stability analysis of inclined two-layer stratified flows, Phys. Fluids, 20(9), 2008.

[16] C. Pozrikidis, Instability of two-layer creeping flow in a channel with parallel-sided walls, J. Fluid Mech., 351, 139-165, 1997.

[17] Lloyd N. Trefethen, Spectral Methods in MATLAB, SIAM, Philadelphia, 2000.

[18] S.A. Thorpe, A method of producing a shear flow in a stratified fluid, J. Fluid Mech., 32(4), 693-704, 1968.

[19] S.A. Thorpe, Experiments on the instability of stratified shear flows: miscrible fluids, J. Fluid Mech., 46(2), 299-319, 1971.

[20] C.S. Yin, Stability of liquid flow down an inclined plane, Phys. Fluids, 6(3), 321-334, 1963.

[21] C.S. Yih, Instability due to viscosity stratification. J. Fluid Mech., 27, 337-352, 1967.

[22] S.G. Yiantsios, B.G. Higgins, Linear stability of plane Poiseuille flow of two superpose fluids, Phys. Fluids, 31(11), 1988.

[23] P. Yecko, S. Zaleski, J.-M. Fullana, Viscous modes in two-phase mixing layers, Phys. Fluids, 14(2), 2002.